Transport analysis and modelling of high radiation and high density plasmas at ASDEX Upgrade

L. Casali, E. Fable, R. Dux, M. Bernert, R. Fischer, A. Kallenbach, B. Kurzan, A. Mlynek, R.M. McDermott, F. Ryter, M. Sertoli, G. Tardini and ASDEX Upgrade Team
Max-Planck-Institut für Plasmaphysik, Boltzmannstraße 2, 85748 Garching, Germany

Future fusion reactors will require high divertor and core radiation by impurity seeding to limit divertor heat loads. In addition, high core densities are required to maximize the fusion power. A well established technique to reduce heat loads on divertor target plates is to insert low and medium Z impurities in the plasma to convert the heat flux into radiation [1]. Radiative cooling by nitrogen have been extensively investigated at ASDEX Upgrade (AUG). Thereby, a confinement increase due to the presence of N has been discovered [2] [3]. The analysis of the transport properties and the radiative power of H-modes under such conditions is presented. Results from the transport analyses taking into account the spatial radiation distribution are reported in [4]. To provide a reliable radiation profile for transport calculations, a non-coronal radiation model using atomic data and experimental profiles was developed and compared to bolometric measurements. A detailed description of the theoretical background and model development can be found in reference [4] as well. The model takes into account that the edge region of H-mode plasmas is modulated by edge-localized modes (ELMs) which lead to a loss of energy and particles from the confined plasma. In the present contribution the modeling results of the evolution of impurities and radiation at the plasma edge, including ELMs, are presented.

Modelling of the radiation and impurity evolution

A time dependent modelling of radiation and impurities in the presence of ELMs has been carried out using the ASTRA transport code [5] coupled to the impurity transport code STRAHL [6]. The codes are run simultaneously at each time step: ASTRA provides the background profiles for STRAHL, which calculates radiation and impurity evolution and then ASTRA uses them to evolve the background profiles to the next time step.

The electron and ion temperatures, as well as the electron density, are modelled in ASTRA, while the impurity density transport and radiation are simulated in STRAHL which takes into account non coronal effects. For the modelling the following facts are essential: in H-mode plasmas the formation of the edge transport barrier (ETB) provides high temperatures and densities leading to a pedestal structure, characterized by very steep edge pressure gradients. These gradients collapse at each ELM crash and recover during inter-ELM phase. All impurities are subject to a neoclassical inward pinch leading to steep impurity density gradients which are flattened during the ELMs. Taking into account all these elements, a semi-empirical transport model is build as follows. In the core T_e and T_i are modeled assuming turbulent + neoclassical transport. In the pedestal both T_e, T_i are modeled assuming the ion neoclassical conductivity. The pedestal is 2.5 cm wide from the separatrix inwards. The boundary conditions are set at the separatrix by experimental values. The evolution of n_e is obtained assuming anomalous transport in the

core and setting $D = const \cdot \chi_i^{NEO}$ in the pedestal. The neoclassical contribution is computed in STRAHL using the NEOART module [7]. Since the particle source in the core is rather small, the convection velocity V is chosen such that the drift parameter fulfills $\frac{-V}{D_n} = \frac{\nabla_{ne}}{n_e}$, D_n being the particle diffusivity. In the pedestal, the convection velocity is set to zero. For the impurities the anomalous part is chosen as a fraction of χ_i while the pedestal is assumed to be at the neoclassical level as indicated by recent finding [8]. The core convection velocity for impurities V_{imp} is derived in the same way as done for the electron convection velocity. The impurities considered in this work are nitrogen (from impurity seeding) and tungsten (from the wall). Their source is set at 2.0 cm outside the separatrix in STRAHL. ELMs are simulated as an instantaneous increase of heat and particle diffusivities in the "ELM affected area" which is 2.5 cm wide. The ELM frequency is set according to the experiments. In the following simulations an ELM lasts for 2 ms and the increase in diffusivity in this duration is adjusted to reproduce the experimental density and stored energy. The diffusive transport during ELMs flattens the profiles which steepen again during the inter ELM phase by the presence of the neoclassical inward pinch.

Modelling results and discussion

Here the modeled radiation characteristics of the N seeded discharge #29254 are presented. Details about this discharge can be found in [1]. This discharge is used as reference discharge. Figure 1 shows the N and W radiation at different radial locations in the pedestal. For N radiation, the outermost location ($\rho_{tor} = 0.98$) emits the highest radiation while for W the innermost ($\rho_{tor} = 0.80$) does. The N radiation from STRAHL is significantly higher than that from corona calculations underlying the importance of the non-coronal effects for low-Z elements at the plasma edge. For W instead, coronal calculations yield the same radiation as STRAHL showing that for high-Z elements coronal equilibrium is a good approximation even at the edge. Interestingly, at the ELM crash, the outermost region of N radiation shows a drop while all other regions experience an increase in P_{rad}. The effects of ELMs on the nitrogen density profile, on its radiative loss function L_Z and radiation are shown in figure 2. Important is to note that despite the flattening of the impurity density profile caused by the ELM, the radiation increases. This behavior can be explained by L_Z which increases at the ELM crash. The radiation enhancement can be understood at the atomic level. Figure d) shows the fractional abundance of N as a function of the radius. The effect of diffusive transport, with which the ELMs are modeled, broadens the shell-like structure of the ionisation stages symmetrically around the local ionisation/recombination balance. The outer region of the ionisation shell is flushed out at the

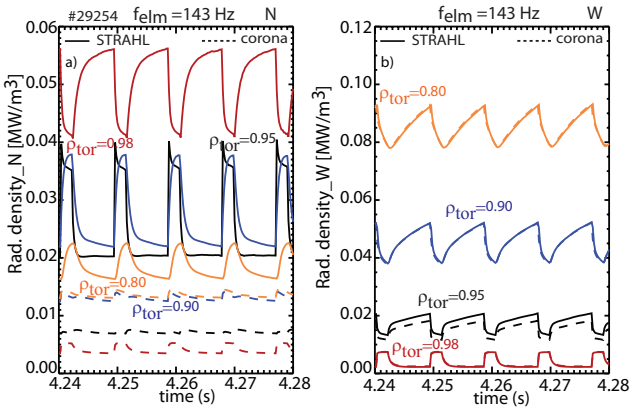

Figure 1: *Modelled radiation from STRAHL at different radial positions in the pedestal. The corresponding dashed lines represent the corona values. a) N radiation; b) W radiation.*

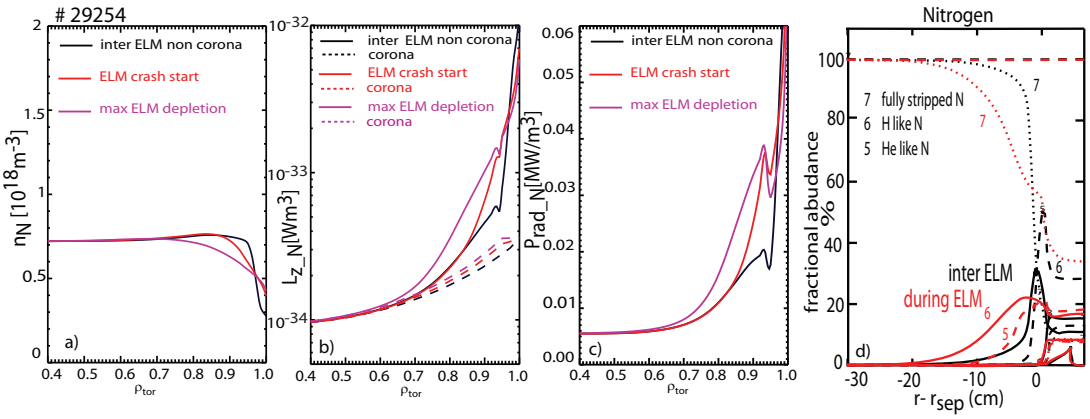

Figure 2: *Effect of ELMs on nitrogen a) density profile; b) L_Z; c) radiation. In dashed the coronal values. d) Fractional abundance of N. The zero point on the x axis represents the separatrix.*

separatrix while the inner region is broadened and shifted radially inwards.

The radiation from impurities depends on their ionisation stage, therefore the inward displacement of the shell leads to higher radiation. Since corona calculations do not take into account the transport effects, the comparison of STRAHL and corona results enables to disentangle the contribution due to the temporal evolution of the n_e and T_e profiles from the transport effects. Moreover, L_Z in corona equilibrium changes only slightly from the inter-ELM phase to during ELMs. This suggests that the transport during the ELM phase dominates the pedestal nitrogen radiation, determining the pedestal evolution of nitrogen.

A scan of f_{ELM} has been performed to investigated the impact on P_{rad} of nitrogen at $\rho_{tor} = 0.98$. The reference discharge has been modelled assuming different ELM frequencies while keeping the total ELM energy loss constant. Here we show the extreme case of 10 Hz: figure 3b) shows that P_{rad} of W increases with decreasing f_{ELM}, while P_{rad} of N, in comparison with figure 1, stays about constant (figure 3a)). This significant increase is reflected in the total radiation and is so high that the simulation crashes (collapse by radiation). This highlights the importance of fast ELMs to prevent W accumulation in the confined region. This finding also in line with previous studies, [9], [10]. The different behavior of N and W can be explained by the difference in density profile peaking of the two impurities. In fact the neoclassical inward pinch in the inter-ELM phase, and therefore the peaking factor, increases with the charge state of the impurity. This means that W has a much more peaked profile compared to N. With high ELM frequency, W has no time to fully develop such a peaked profile. With low ELMs frequencies the strong peaked profile results in high W accumulation. Moreover, one can notice that, in the analysed frequency range [10-200 Hz], nitrogen radiation at $\rho_{tor} = 0.98$ reaches about the steady state at the end of the ELM cycle. This suggests that P_{rad} of N is not determined by the ELM frequency but is only modulated by it. The fact that the outer region of tungsten radiation does not saturate while the nitrogen radiation does, indicates that W radiation depends directly on the ELM frequency while N does not. In order to compare the modelled radiated power with P_{rad} measured by diode bolometers, the STRAHL radiation has been integrated along the experimental lines of sight (LOS), with some care in avoiding lines of sight looking into the divertor. Both STRAHL

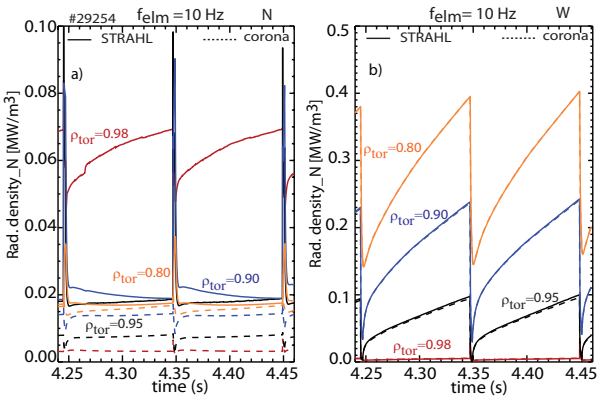

Figure 3: *a) 10 Hz case: N radiation; b) W radiation; The dashed lines represent the corona values.*

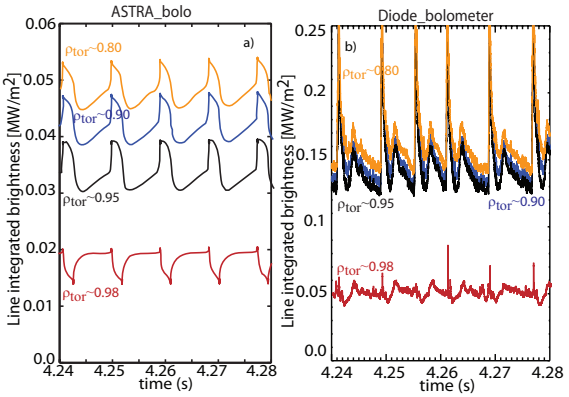

Figure 4: *a) Integrated radiation from STRAHL along LOS of real camera. (b) Radiation from diode bolometer.*

P_{rad} ((figure 4a)) and diode bolometers (figure 4b)) exhibit a radiation peak at the ELM crash except at $\rho_{tor} = 0.98$ where a drop occurs. The diode signals at $\rho_{tor} = 0.98$ detect small spikes before the drop also visible in the model. At the other radial locations the diodes detect more pronounced peaks compared to $\rho_{tor} = 0.98$. It should be pointed out that the lines of sight at the high field side make a longer path in the scrape of layer (SOL) compared to the lines of sights at the low field side (used for $\rho_{tor} = 0.98$). The SOL region is characterized by high radiation which is not taken into account in the model. Therefore, the possible role of the SOL is under investigation. The modelled P_{rad} is about a factor of 3 smaller than the measured one. However, one has to keep in mind that the diodes at AUG suffer of wavelength responsivity and lack of sensitivity [11]. The comparison with the diodes needs further investigations, but already at this stage it shows that the diffusive ELM modelling can reproduce the temporal evolution of P_{rad}.

Acknowledgements

This project has received funding from the Euratom research and training programme 2014-2018.

References

[1] A. Kallenbach et al., Plasma Phys. Control. Fusion **55** 124041 (2013)
[2] J. Schweinzer et al., Nucl. Fusion **51** 113003 (2011)
[3] G. Tardini et al., Plasma Phys. Control. Fusion **55** 015010 (2012)
[4] L. Casali et al., accepted in EPJ web of Conferences, 3rd European Energy Conf. (2013)
[5] E. Fable et al., Plasma Phys. Control. Fusion **55** 074007 (2013)
[6] R. Dux, STRAHL anual IPP report **10/30** (2006)
[7] A. Peeters, Phys. Plasmas 7(1), 268-275 (200)
[8] T. Pütterich et al., Journal of Nuclear Materials **415** S334 (2011)
[9] T. Pütterich et al., 36th EPS on Plasma Phys. (2009)
[10] R. Dux et al., Nucl. Fusion 51 053002 (2011)
[11] M. Bernert et al., Review of scientific Instruments 85 033503 (2014)